

MATHEMATICAL ANALYSIS OF RUBELLA DISEASE DYNAMICS: THE ROLE OF VERTICAL TRANSMISSION AND VACCINATION

Sunday Olumuyiwa Adewale¹, Temitayo Olabisi Oluyo², Lawal Wasiu Olaitan^{3*},
Janet Kikelomo Oladejo⁴

¹⁻⁴Department of Pure and Applied Mathematics, Ladoke Akintola
University of Technology, PMB 4000, Ogbomosho, Oyo State, Nigeria

E-mail: ¹⁾ soadewale@lautech.edu.ng, ²⁾ tooluyo@lautech.edu.ng,
³⁾ wolawal90@pgschool.lautech.edu.ng, ⁴⁾ jkoladejo@lautech.edu.ng

Abstract

Rubella known as German measles constitutes a significant threat to global health, as every individual in the human population is vulnerable to its highly contagious and severe effects. The risk of congenital rubella syndrome is significantly elevated when pregnant women contract the virus, transmitting it to the fetus. This research develops and examines a mathematical framework to simulate rubella's transmission patterns. The model categorizes the population into seven distinct compartments: Susceptible individuals $S(t)$, Vaccinated individuals $V(t)$, Persons with lifelong immunity after receiving a second vaccine dose $P(t)$, Infected individuals $I(t)$, Treated individuals $T(t)$, Recovered individuals $R(t)$. A detailed examination of the model's qualitative features is presented, the formulated model was shown to have non-negative solutions in feasible regions of human population. Furthermore, the model has a stable disease-free equilibrium if the basic reproduction number R_0 is less than unity, unstable otherwise. Computational experiments were performed using MATLAB R2013a to examine the effects of critical parameters on rubella transmission, yielding insightful graphical representations. Simulation studies revealed that reducing contact and vertical transmission rates, while increasing recovery rates, vaccination rates (first and second doses), and maternal immunization, are vital for mitigating rubella's impact in the population.

Keywords: Epidemiological Model, Rubella, Equilibrium Point, Basic Reproduction Number, Stability, Simulations

1. INTRODUCTION

Rubella, a highly contagious viral infection, poses significant health risks globally, particularly to pregnant women and unborn children (Vueba & do Céu Sousa, 2020). Despite the availability of effective vaccines, rubella remains a significant concern globally due to lacking of surveillance systems and national incidence figures in many parts of the world (Prawoto et al., 2020). According to the World Health Organization (WHO), approximately 26,000 cases of rubella occur annually worldwide, primarily in Asia, Africa, and the Middle East (World Health Organization, 2011).

The consequences of rubella infection can be severe, especially for pregnant women, with up to 90% of infants born to mothers infected during the first 12 weeks of pregnancy developing congenital rubella syndrome (CRS) (Gong et al., 2024; Tilahun et al., 2022). CRS can lead to growth delays, deafness, cataracts, congenital heart defects, and problems with mental development and learning (Amelia & Tasman, 2021). These

complications underscore the importance of understanding rubella transmission dynamics and evaluating effective control measures.

Mathematical modeling of infectious diseases has proven essential in understanding disease transmission dynamics and evaluating control measures (Castillo-Chavez & Song, 2004). Mathematical models can simulate the spread of disease, predict outbreak patterns, and assess the impact of intervention strategies. Previous studies have developed mathematical models for rubella transmission, incorporating vaccination and vertical transmission (Duru et al., 2023; Tilahun et al., 2022).

Vertical transmission, where the virus is passed from mother to child during pregnancy, plays a critical role in rubella epidemiology. This mode of transmission can lead to severe complications, including CRS (Bhattacharjee & Jain, 2024). Understanding the dynamics of vertical transmission is crucial for developing effective control strategies. Vaccination remains the most effective method for preventing rubella infection and CRS (Tilahun et al., 2022).

Despite the availability of effective vaccines, rubella persists in many regions due to factors such as vaccine hesitancy, inadequate healthcare infrastructure, and lack of awareness (Abdullahi & Sime, 2018; Adewumi et al., 2013). In Africa, specifically, the lack of surveillance systems and national incidence figures hinders effective control measures. This study aims to develop a mathematical model for rubella disease dynamics, focusing on the role of vertical transmission and vaccination.

Building upon existing research, this study will contribute to the understanding of rubella transmission dynamics and evaluate the impact of vaccination and vertical transmission on disease control. The findings of this study will inform public health policy and guide intervention strategies to reduce the burden of rubella.

2. MATHEMATICAL MODEL

2.1. Model formulation

At time t , the total human population denoted by $N(t)$, is divided into seven distinct groups: the Susceptible, $S(t)$, (individuals vulnerable to rubella), Vaccinated $V(t)$, (those who received the first vaccine dose), Protected $P(t)$, (individuals with lifelong immunity after receiving the second dose of vaccine), Exposed $E(t)$, (individuals who contacted infected persons), Infected $I(t)$, (represent those showing symptoms of rubella illness), Treated $T(t)$ (consist of infected individuals undergoing treatment) and Recovered $R(t)$, (represent individuals with temporary immunity).

2.2. Population Dynamics

The susceptible class $S(t)$, increases through recruitment into the population at a rate of π , waning out of first dose of vaccination at a rate of ξ as well as rate of loss of immunity due to recovery ϵ and decreases by delivering the first vaccine dose at a rate of σ and contact with infected individuals at a rate of β . Vaccinated class, $V(t)$, increases when the first dose of vaccine is received by individual in the susceptible class at a rate σ as well as maternal vaccination rate ϕ observed before pregnancy but decreases at a rate of ω , when second-dose vaccination is received and entering into the susceptible class due to waning out at a rate of ξ . Also, the protected class, $P(t)$, increases when the second dose of vaccine is received at the rate of ω . Exposed class, $E(t)$, increases when the

susceptible class contact with infected individuals at a rate of β decreases through individual moving to the infected class at a rate of α . The infected class, $I(t)$, due to progression of individual from the exposed class at a rate of α and vertical transmission rate θ and decreases through induced death at a rate of δ as well as undergoing treatment at a rate of γ . Treated class, $T(t)$, increases through individual isolated and receives treatment at a rate of γ and decreases by disease induce death at a rate of δ and recovery at a rate of τ . The recovered class $R(t)$, increases through inflow of individual from treatment class at a rate of τ and decreases through temporary immunity loss. Natural mortality affects each group, resulting in a decline at a rate of μ .

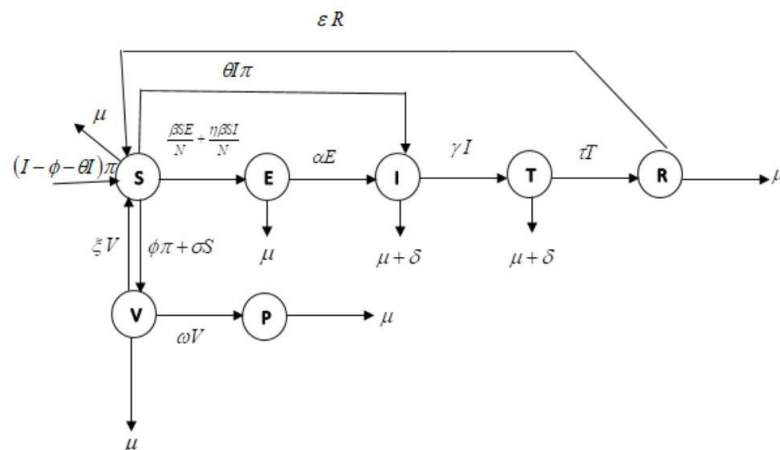


Figure 1. Rubella Disease Model Diagram

Using the flow diagram, figure 1 and the dynamics of the disease as described above, the proposed model is mathematically expressed through ordinary differential equations, incorporating the conventional incidence rate structure as given in Equation (1).

$$\begin{aligned} \frac{dS}{dt} &= (1 - \phi - \theta I)\pi - \frac{\beta SE}{N} - \frac{\eta BSI}{N} - (\mu + \sigma)S + \varepsilon R + \xi V \\ \frac{dV}{dt} &= \phi\pi + \sigma S - (\mu + \xi + \omega)V \\ \frac{dP}{dt} &= \omega V - \mu P \\ \frac{dE}{dt} &= \frac{\beta SE}{N} + \frac{\eta BSI}{N} - (\mu + \alpha)E \\ \frac{dI}{dt} &= \alpha E + \theta I\pi - (\mu + \gamma + \delta)I \\ \frac{dT}{dt} &= \gamma I - (\mu + \tau + \delta)T \\ \frac{dR}{dt} &= \tau T - (\mu + \varepsilon)R \end{aligned} \quad (1)$$

For simplicity, we let

$$\begin{aligned} k_1 &= (\sigma + \mu) \\ k_2 &= (\mu + \xi + \omega) \\ k_3 &= (\mu + \alpha) \end{aligned}$$

$$\begin{aligned} k_4 &= (\mu + \gamma + \delta) \\ k_5 &= (\mu + \tau + \delta) \\ k_6 &= (\mu + \varepsilon) \end{aligned}$$

The force of infection is given as

$$\lambda^* = \frac{\beta SE}{N} + \frac{\eta \beta SI}{N} \quad (2)$$

Table 1. The Description of Parameters

Parameters	Description (rate)	Reference value	Source
π	Recruitment	0.15	Getachew <i>et al.</i>
σ	First Vaccination	0.3	Getachew <i>et al.</i>
ϕ	Maternal Vaccination	0.6	Assumed
ε	Loss of Immunity due to recovery	0.4	Assumed
θ	Vertical transmission	0.55	Getachew <i>et al.</i>
τ	Recovery	0.15	Assumed
β	Contact	0.4	Getachew <i>et al.</i>
γ	Treatment	0.4	Getachew <i>et al.</i>
ξ	Waning out of first vaccination	0.6	Getachew <i>et al.</i>
η	Modification parameter	0.5	Assumed
μ	Natural death	0.4	Getachew <i>et al.</i>
δ	Disease Induced death	0.08	Getachew <i>et al.</i>
α	Progression	0.85	Getachew <i>et al.</i>
ω	Second vaccination	1	Getachew <i>et al.</i>

3. ANALYSIS OF THE MODEL

3.1. Positivity and boundedness of solutions of the model

Theorem 1: Given non-negative initial values $S(0)$, $V(0)$, $P(0)$, $E(0)$, $I(0)$, $T(0)$, and $R(0)$ in Ω , the solution set $\{S(t), V(t), P(t), E(t), I(t), T(t), R(t)\}$ preserves non-negativity in Ω for all $t \geq 0$

Proof: By examining equation (1) of the model, we observe that

$$\frac{dS}{dt} > -\frac{\beta SE}{N} - \frac{\eta \beta SI}{N} - (\mu + \sigma)S \quad (3)$$

rearranging and integrating equation (3) produces

$$\begin{aligned} \ln S(t) &\geq -\int \left(\frac{\beta(E+\eta I)}{N} + (\mu + \sigma) \right) dt & S(t) = \\ S(0) \exp &^{-\left(\frac{\beta(E+\eta I)}{N} + (\mu + \sigma) \right) t} & (4) \end{aligned}$$

It follows that $S(t) \geq 0$ holds true only when $S(0) \geq 0$. Analogous reasoning applies to the remaining state variables, ensuring their non-negativity. Consequently, non-negative initial conditions guarantee non-negative state variables for all $t \geq 0$.

Theorem 2: For the system modeled by $\Omega = \left\{ (S(t), V(t), P(t), E(t), I(t), T(t), R(t)) \in R_+^7 : N(t) \leq \frac{\pi}{\mu} \right\}$ are positively invariant.

Proof: Consider the total human population $N(t)$ at a given time t , as $N(t) = S(t) + V(t) + P(t) + E(t) + I(t) + T(t) + R(t)$ (5)

Differentiating (5) with respect to t gives

$$\frac{dN}{dt} = \frac{dS}{dt} + \frac{dV}{dt} + \frac{dP}{dt} + \frac{dE}{dt} + \frac{dI}{dt} + \frac{dT}{dt} + \frac{dR}{dt} \quad (6)$$

Putting the derivative from (1) reduces (6) to

$$\begin{aligned} \frac{dN}{dt} &= \pi - (E + I)\delta - \mu N \\ \frac{dN}{dt} &\leq \pi - \mu N \quad (7) \end{aligned}$$

Integrating both sides of (7)

$$N(t) \leq N(0)e^{-\mu t} + \frac{\pi}{\mu}(1 - e^{-\mu t}) \quad (8)$$

Analyzing limits as t approaches 0 and infinity reveals $N(t)$ approaches $N(0)$ and π/μ . Hence, $0 \leq N(t) \leq \pi/\mu$. This demonstrates model (1) solutions are non-negative and bounded within Ω for all $t \geq 0$, ensuring epidemiological realism and mathematical coherence.

3.2. Rubella-free equilibrium point (DFE)

Model (1) equilibrium points are characterized by constant solutions that fulfill

$$\begin{aligned} \frac{dS}{dt} = \frac{dV}{dt} = \frac{dP}{dt} = \frac{dE}{dt} = \frac{dI}{dt} = \frac{dT}{dt} = \frac{dR}{dt} &= 0 \quad (9) \\ S \neq 0, V \neq 0, P \neq 0, E = 0, I = 0, T = 0, R = 0 & \quad (10) \end{aligned}$$

The disease-free equilibrium ε_0 , obtained by solving system (1) subject to (10) as

$$\varepsilon_0 = \left(\frac{\pi(k_2(1-\varphi)+\xi\varphi)}{Nk_2+\sigma(\mu+\omega)}, \frac{\pi k_2(\mu\varphi+\sigma)}{\mu k_2(\mu(k_2+\sigma)+\omega\sigma)}, \frac{\pi w k_2(\mu\varphi+\sigma)}{\mu k_2(\mu(k_2+\sigma)+\omega\sigma)}, 0, 0, 0, 0 \right) \quad (11)$$

3.3. Basic Reproduction Number R_0

The basic reproduction number R_0 , is the average number of secondary cases of the disease made by a typical infectious person during his infectious period in a complete susceptible population. Using the next generation operator approach described by Diekmann et al. (1990); Van den Driessche and Watmough (2002).

$$R_0 = \rho(FV^{-1}) \quad (12)$$

At equilibrium ε_0 , F signifies the transmission Jacobian given by

$$F = \begin{pmatrix} \frac{\mu\beta(k_2(1-\varphi)+\xi\varphi)}{\mu k_2+\sigma(\mu+\omega)} & \frac{\eta\mu\beta(k_2(1-\varphi)+\xi\varphi)}{\mu k_2+\sigma(\mu+\omega)} \\ 0 & 0 \end{pmatrix} \quad (13)$$

Here, V denotes the transition Jacobian evaluated at ε_0

$$V = \begin{pmatrix} k_3 & 0 \\ \alpha(k_4 - \theta\pi) & \end{pmatrix} \quad (14)$$

Using (12), the basic reproduction number is the largest dominant spectral radius of the FV^{-1} is computed as

$$R_0 = \frac{\mu\beta(k_2(1-\varphi)+\xi\varphi)(k_4+\eta\alpha-\theta\pi)}{k_3(k_4-\theta\pi)(\mu k_2+\sigma(\mu+\omega))} \quad (15)$$

3.4. Rubella endemic equilibrium ε_e

The human population is said to be in a state of rubella-endemic equilibrium ε_e , when

$$S(t) \neq V(t) \neq P(t) \neq E(t) \neq I(t) \neq T(t) \neq R(t) \neq 0 \quad (16)$$

Solving (1) subject to (16)

$$\varepsilon_e = (S^*, V^*, P^*, E^*, I^*, T^*, R^*) \quad (17)$$

Where

$$\begin{aligned} S^* &= \frac{\pi k_3 k_5 k_6 (k_4 - \theta\pi)(k_2(1-\varphi) + \xi\varphi)}{k_5 k_6 (\pi\alpha\lambda^* \theta k_2 + k_2 k_3 (k_4 - \theta\pi)(\lambda^* + k_1) - k_3 (k_4 - \theta\pi)\xi\sigma) - \alpha\gamma\lambda^* \tau k_2 \varepsilon} \\ V^* &= \frac{\pi (\varphi k_5 k_6 (\pi\alpha\lambda^* \theta k_2 + \varphi k_3 (k_4 - \theta\pi)(k_2(\lambda^* + k_1) - \xi\sigma) - \alpha\gamma\lambda^* \tau k_2 \varepsilon\varphi) + \sigma k_3 k_5 k_6 (k_4 - \theta\pi)(k_2(1-\varphi) + \xi\varphi))}{k_2} \\ P^* &= \frac{\pi\omega (\varphi k_5 k_6 (\pi\alpha\lambda^* \theta k_2 + \varphi k_3 (k_4 - \theta\pi)(k_2(\lambda^* + k_1) - \xi\sigma) - \alpha\gamma\lambda^* \tau k_2 \varepsilon\varphi) + \sigma k_3 k_5 k_6 (k_4 - \theta\pi)(k_2(1-\varphi) + \xi\varphi))}{\mu k_2} \\ E^* &= \frac{\pi\lambda^* k_5 k_6 (k_4 - \theta\pi)(k_2(1-\varphi) + \xi\varphi)}{k_5 k_6 (\pi\alpha\lambda^* \theta k_2 + k_2 k_3 (k_4 - \theta\pi)(\lambda^* + k_1) - k_3 (k_4 - \theta\pi)\xi\sigma) - \alpha\gamma\lambda^* \tau k_2 \varepsilon} \\ I^* &= \frac{\pi\alpha\lambda^* k_5 k_6 (k_2(1-\varphi) + \xi\varphi)}{k_5 k_6 (\pi\alpha\lambda^* \theta k_2 + k_2 k_3 (k_4 - \theta\pi)(\lambda^* + k_1) - k_3 (k_4 - \theta\pi)\xi\sigma) - \alpha\gamma\lambda^* \tau k_2 \varepsilon} \\ T^* &= \frac{\pi\alpha\gamma\lambda^* k_6 (k_2(1-\varphi) + \xi\varphi)}{k_5 k_6 (\pi\alpha\lambda^* \theta k_2 + k_2 k_3 (k_4 - \theta\pi)(\lambda^* + k_1) - k_3 (k_4 - \theta\pi)\xi\sigma) - \alpha\gamma\lambda^* \tau k_2 \varepsilon} \\ R^* &= \frac{\pi\alpha\gamma\lambda^* \tau (k_2(1-\varphi) + \xi\varphi)}{k_5 k_6 (\pi\alpha\lambda^* \theta k_2 + k_2 k_3 (k_4 - \theta\pi)(\lambda^* + k_1) - k_3 (k_4 - \theta\pi)\xi\sigma) - \alpha\gamma\lambda^* \tau k_2 \varepsilon} \end{aligned} \quad (18)$$

Substituting E^* and I^* into (2) gives

$$\lambda^* = \frac{\mu\beta\lambda^*k_5k_6(k_2(1-\varphi)+\xi\varphi)(k_4+\alpha-\theta\pi)}{k_5k_6(\pi\alpha\lambda^*\theta k_2+k_2k_3(k_4-\theta\pi)(\lambda^*+k_1)-k_3(k_4-\theta\pi)\xi\sigma)-\alpha\gamma\lambda^*\tau k_2\varepsilon} \quad (19)$$

Solving (19) gives

$$\lambda^* = \frac{k_3k_5k_6(k_4-\theta\pi)(\mu k_2+\sigma(\mu+\omega))(R_0-1)}{\pi\alpha\theta k_2k_5k_6+k_2k_3k_5k_6(k_4-\theta\pi)-\alpha\gamma\tau k_2\varepsilon} \quad (20)$$

Provided $R_0 > 1$, $k_4 > \theta\pi$, and $\pi\alpha\theta k_2k_5k_6 + k_2k_3k_5k_6(k_4 - \theta\pi) > \alpha\gamma\tau k_2\varepsilon$; then there exist a unique rubella-endemic equilibrium point.

3.5. Local stability of rubella-free equilibrium point

Theorem 3: The local stability of disease-free equilibrium of the system (1) exists when $(R_0) < 1$. Otherwise, it is unstable.

Proof: In order to determine the local stability of rubella-free equilibrium, the Jacobian matrix of system (1) evaluated at ε_0 is examined as;

$$J_{\varepsilon_0} = \begin{pmatrix} -k_1 - \lambda & \xi & 0 & \frac{-\mu\beta(k_2(1-\varphi)+\xi\varphi)}{\mu k_2 + \sigma(\mu + \omega)} & \frac{-\eta\mu\beta(k_2(1-\varphi)+\xi\varphi)}{\mu k_2 + \sigma(\mu + \omega)} & 0 & \varepsilon \\ \sigma & -k_2 - \lambda & 0 & 0 & 0 & 0 & 0 \\ 0 & \omega & -\mu - \lambda & 0 & 0 & 0 & 0 \\ 0 & 0 & 0 & \frac{\mu\beta(k_2(1-\varphi)+\xi\varphi)}{\mu k_2 + \sigma(\mu + \omega)} - k_3 - \lambda & \frac{\eta\mu\beta(k_2(1-\varphi)+\xi\varphi)}{\mu k_2 + \sigma(\mu + \omega)} & 0 & 0 \\ 0 & 0 & 0 & \alpha & -(k_4 - \theta\pi) - \lambda & 0 & 0 \\ 0 & 0 & 0 & 0 & \gamma & -k_5 - \lambda & 0 \\ 0 & 0 & 0 & 0 & 0 & \tau & -k_6 - \lambda \end{pmatrix} \quad (21)$$

This has eigenvalue $\lambda = -k_1, \lambda = -k_2, \lambda = -k_5, \lambda = -k_6, \lambda = -\mu$

Others are obtained from the roots of characteristic equation

$$\lambda^2 + \lambda A_1 + A_2 = 0 \quad (22)$$

Where

$$A_1 = k_3 + (k_4 - \theta\pi) - \frac{\mu\beta(k_2(1-\varphi)+\xi\varphi)}{\mu k_2 + \sigma(\mu + \omega)}$$

$$A_2 = k_3(k_4 - \theta\pi)(1 - R_0) \quad (23)$$

Now, if $k_4 > \theta\pi$, $k_3 + (k_4 - \theta\pi) > \frac{\mu\beta(k_2(1-\varphi)+\xi\varphi)}{\mu k_2 + \sigma(\mu + \omega)}$ and R_0 is less than unity, then (22) has negative roots with negative real parts. Hence, the rubella-free equilibrium is locally asymptotically stable. Otherwise, it is unstable.

3.6. Global stability of rubella-free equilibrium point

We established two necessary conditions for global stability of disease-free equilibrium, as obtained in Castillo-Chavez and Song (2004) to demonstrate global stability of the rubella-free equilibrium when $R_0 < 1$.

We start by re-writing system (1) in the form

$$\begin{aligned} \frac{dX}{dt} &= F(X, Z) \\ \frac{dZ}{dt} &= G(X, Z), G(X, 0) = 0 \end{aligned} \quad (24)$$

Where

$X = (S(t), V(t), P(t), R(t))$ and $Z = (E(t), I(t), T(t))$ depict the system's uninfected and infected states, $F(X, Z)$ and $G(X, Z)$ correspond to the right-hand expressions of $\frac{dX}{dt}$ and $\frac{dZ}{dt}$, when the variables $E(t)$, $I(t)$, and $T(t)$ are initialized to zero.

Now, from (24), one has;

$$F(X, Z) = \begin{pmatrix} (1 - \varphi - \theta I)\pi - \frac{\beta SE}{N} - \frac{\eta \beta SI}{N} - (\mu + \sigma)S + \varepsilon R + \xi V \\ \varphi\pi + \sigma S - (\mu + \xi + \omega)V \\ \omega V - \mu P \\ \tau T - (\mu + \varepsilon)R \end{pmatrix}$$

Consider $X^* = (S(t), V(t), P(t), R(t))$ as the equilibrium of system (24), we establish the following.

Theorem 4: Global asymptotic stability of the rubella-free equilibrium ε_0 , in system (1) holds if $R_0 < 1$; given the satisfaction of supplementary conditions H_1 and H_2 .

$$H_1: \frac{dX}{dt} = F(X, 0), X^* \text{ is globally asymptotically stable;}$$

$$H_2: G(X, Z) = AZ - G(X, Z) \leq 0, \hat{G}(X, Z) \geq 0 \text{ for } (X, Z) \in \Omega$$

We define $A = \frac{\partial G}{\partial Z}$, a Metzler matrix with non-negative off-diagonal entries, and Ω as the domain of biological feasibility.

Proof: Global asymptotic stability of X^* is proven by examining the long-term dynamics of the reduced system (24) and taking the limit as $t \rightarrow \infty$

$$\begin{aligned} \frac{dX}{dt} &= F(X, 0) \text{ implies that} \\ \frac{dS}{dt} &= (1 - \varphi)\pi - (\mu + \sigma)S + \varepsilon R + \xi V \\ \frac{dV}{dt} &= \varphi\pi + \sigma S - (\mu + \xi + \omega)V \\ \frac{dP}{dt} &= \omega V - \mu P \\ \frac{dR}{dt} &= -(\mu + \varepsilon)R \end{aligned} \quad (25)$$

Solving (25) gives

$$\begin{aligned} S(t) &= S(0)e\{-(\mu + \sigma)t\} + \frac{\pi k_2(1-\varphi)+\xi\varphi}{\mu k_2+\sigma(\mu+\omega)} (1 - \{-(\mu + \sigma)t\}) + \varepsilon R(0)e\{-(\mu + \varepsilon)t\} \\ V(t) &= V(0)e\{-(\mu + \xi + \omega)t\} + \frac{\pi k_2(\mu\varphi+\gamma)}{k_2(\mu k_2+\sigma(\mu+\omega))} (1 - e\{-(\mu + \xi + \omega)t\}) \\ P(t) &= P(0)e\{-\mu t\} + \frac{\pi\omega k_2(\mu\varphi+\sigma)}{\mu k_2(\mu(k_2+\sigma)+\omega\sigma)} (1 - e\{-\mu t\}) \quad (26) \quad R(t) = R(0)e\{-(\mu + \varepsilon)t\} \end{aligned}$$

Taking the limit of (26) as $t \rightarrow \infty$

$$S(t), V(t), P(t), R(t) \rightarrow \left(\frac{\pi k_2(1-\varphi)+\xi\varphi}{\mu k_2+\sigma(\mu+\omega)}, \frac{\pi k_2(\mu\varphi+\gamma)}{k_2(\mu k_2+\sigma(\mu+\omega))}, \frac{\pi\omega k_2(\mu\varphi+\sigma)}{\mu k_2(\mu(k_2+\sigma)+\omega\sigma)}, 0 \right) \quad (27)$$

This shows that initial conditions do not influence the system dynamics, In essence, all trajectories starting in Ω asymptotically approach $X^* = \varepsilon_0$, as $t \rightarrow \infty$. Consequently, the equilibrium X^* exhibits global asymptotic stability for the dynamical system $\frac{dX}{dt} = F(X, 0)$. Furthermore, we show that

$$H_2: G(X, Z) = AZ - \hat{G}(X, Z), \hat{G}(X, Z) \geq 0 \text{ for } (X, Z) \in \Omega$$

From system (1)

$$G(X, Z) = \begin{pmatrix} \frac{\beta SE}{N} + \frac{\eta\beta SI}{N} - (\mu + \alpha)E \\ \alpha E + \theta I\pi - (\mu + \gamma + \delta)I \\ \gamma I - (\mu + \tau + \delta)T \end{pmatrix}$$

$$A = \frac{\partial G}{\partial Z}(X^*, 0) = \begin{pmatrix} \frac{\beta S}{N} - (\mu + \alpha)\frac{\eta\beta S}{N} & 0 \\ \alpha\theta\pi - (\mu + \gamma + \delta) & 0 \\ 0 & \gamma(\mu + \tau + \delta) \end{pmatrix}$$

$$AZ = \begin{pmatrix} \frac{\beta S}{N} - (\mu + \alpha)\frac{\eta\beta S}{N} & 0 \\ \alpha\theta\pi - (\mu + \gamma + \delta) & 0 \\ 0 & \gamma(\mu + \tau + \delta) \end{pmatrix} \begin{pmatrix} E \\ I \\ T \end{pmatrix}$$

Then $\hat{G}(X, Z) = AZ - G(X, Z)$, so that

$$\hat{G}(X, Z) = \begin{pmatrix} \left(\frac{\beta E}{N} + \frac{\eta\beta I}{N} \right) \left(\frac{\pi k_2(1-\varphi)+\xi\varphi}{\mu k_2+\sigma(\mu+\omega)} - S \right) \\ 0 \\ 0 \end{pmatrix} \quad (28)$$

Obviously $\hat{G}(X, Z) \geq 0$, since $\frac{\pi k_2(1-\varphi)+\xi\varphi}{\mu k_2+\sigma(\mu+\omega)} > S$ at any time t , as shown in H_1 .

Now, it has being established that:

$H_1: \frac{dX}{dt} = F(X^*, 0)$, X^* is globally asymptotically stable

$H_2: G(X, Z) = AZ - \hat{G}(X, Z), \hat{G}(X, Z) \geq 0$ for all biologically feasible states $(X, Z) \in \Omega$. This condition ensures global asymptotic stability of ε_0 if $R_0 < 1$, otherwise, instability prevails.

3.7. Global stability of Endemic Equilibrium Point

Asymptotic global stability of the endemic prevalence equilibrium is analyzed using the approach of Adepoju & Ibrahim (2024).

Theorem 5: The endemic equilibrium point ε_e^* is globally asymptotically stable whenever $R_0 > 1$.

Proof: Consider the Lyapunov function $Q: \Omega \in R_+^7 \rightarrow R_+$ defined by

$$Q = \frac{1}{2}[(S - S^*) + (V - V^*) + (P - P^*) + (E - E^*) + (I - I^*) + (T - T^*) + (R - R^*)]^2 \quad (29)$$

Temporal differentiation of equation (29) yields

$$\dot{Q} = [(S - S^*) + (V - V^*) + (P - P^*) + (E - E^*) + (I - I^*) + (T - T^*) + (R - R^*)] \left(\frac{dS}{dt} + \frac{dV}{dt} + \frac{dP}{dt} + \frac{dE}{dt} + \frac{dI}{dt} + \frac{dT}{dt} + \frac{dR}{dt} \right)$$

$$= [(S - S^*) + (V - V^*) + (P - P^*) + (E - E^*) + (I - I^*) + (T - T^*) + (R - R^*)][\pi - \mu(S + V + P + E + I + T + R) - (I + T)\delta]$$

$$\dot{Q} \leq [(S - S^*) + (V - V^*) + (P - P^*) + (E - E^*) + (I - I^*) + (T - T^*) + (R - R^*)](\pi - \mu(S + V + P + E + I + T + R))$$

$$\dot{Q} \leq -\mu[(S - S^*) + (V - V^*) + (P - P^*) + (E - E^*) + (I - I^*) + (T - T^*) + (R - R^*)] \left((S + V + P + E + I + T + R) - \frac{\pi}{\mu} \right)$$

$$\dot{Q} \leq -\mu[(S - S^*) + (V - V^*) + (P - P^*) + (E - E^*) + (I - I^*) + (T - T^*) + (R - R^*)](S + V + P + E + I + T + R - (S^* + V^* + P^* + E^* + I^* + T^* + R^*))$$

$$\dot{Q} \leq -\mu[(S - S^*) + (V - V^*) + (P - P^*) + (E - E^*) + (I - I^*) + (T - T^*) + (R - R^*)]^2$$

$$\dot{Q} \leq 0 \text{ with } \dot{Q} = 0 \text{ iff } S = S^*, V = V^*, P = P^*, E = E^*, I = I^*, T = T^*, R = R^*$$

As a result, the endemic equilibrium defines the largest invariant set within the feasible region. According to LaSalle's invariance principle, uniqueness guarantees global asymptotic stability if $R_0 > 1$. Otherwise, the equilibrium is unstable.

3.8. Result of Sensitivity Index

This section examined the rubella model's robustness by conducting sensitivity analysis on the basic reproduction number. We identified critical parameters significantly influencing the model using the normalized forward sensitivity index as applied in Oluyo and Adeyemi (2018).

This approach reveals how variations in parameter values impact the model's effectiveness. With this methodology, the normalized forward sensitivity index of R is formally defined, displaying a differential sensitivity to parameter ρ as

$$X_{\rho}^{R_0} = \frac{\partial R_0}{\partial \rho} \times \frac{\rho}{R_0} \quad (29)$$

To illustrate this concept, the recruitment rate π effects on R_0 is assessed via sensitivity index. as

$$X_{\pi}^{R_0} = \frac{\theta\eta\alpha\pi}{(\gamma+\delta+\mu-\theta\pi)(\gamma+\delta+\mu+\eta\alpha-\theta\pi)}$$

$$X_{\pi}^{R_0} = 0.0534$$

Table 2 presents the sensitivity indices for R_0 concerning additional parameters, using reference values. The results reveal that contact rate β has the highest sensitivity. Other parameters, including θ and maternal vaccination rate ϕ , also demonstrate substantial sensitivity. The sensitivity index value, $X_{\rho}^{R_0} = 0.0534$ signifies that a 10% increase (or decrease) in π leads to a corresponding 0.534% increase (or decrease) in R_0 . Similarly, the sensitivity indices for other parameters are interpreted in the same way.

Table 2. Sensitivity indices of R_0 to its associated parameter

Parameters	Sensitivity indices
π	0.0534
σ	-0.3443
θ	0.0534
β	1
γ	-0.2588
ξ	0.2648
μ	-0.3102
δ	-0.0518
α	-0.1641
ω	-0.1892
ϕ	-0.5385

4. NUMERICAL SIMULATIONS AND DISCUSSION

Simulation results for the rubella model (1) are discussed, focusing on dynamic behavior, stability, and parameter sensitivity, obtained using Maple 18.0. Parameter values used in simulations were sourced from available literature, with estimates made for unavailable data, as presented in Table 1.

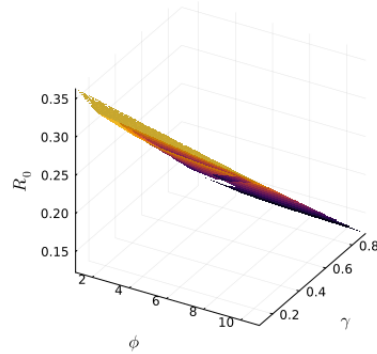


Figure 2. Sensitivity of R_0 to the parameters ϕ and γ

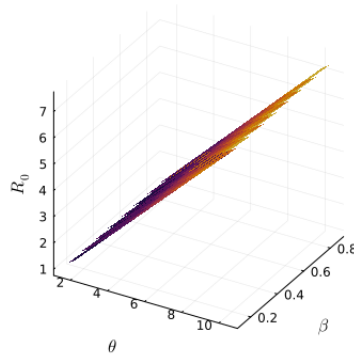


Figure 3. Sensitivity of the basic reproduction number to the parameters β and θ

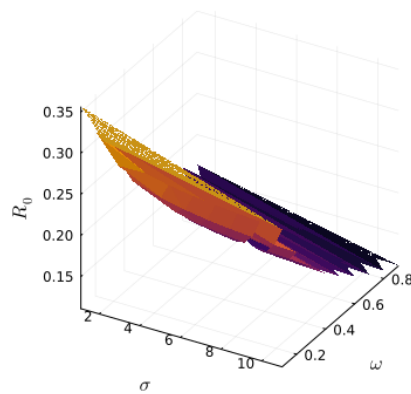


Figure 4. Sensitivity evaluation of R_0 with respect to parameters σ and ω

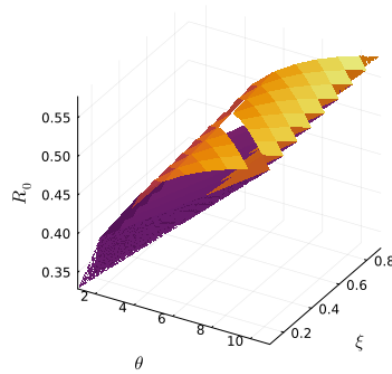


Figure 5. Sensitivity of the basic reproduction number to the parameters θ and ξ

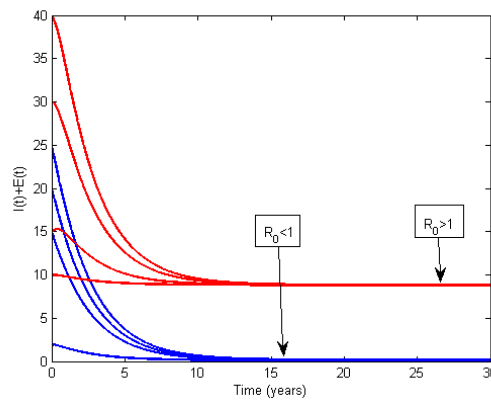


Figure 6. Global asymptotic stability of both endemic and disease-free equilibria of infectious human population

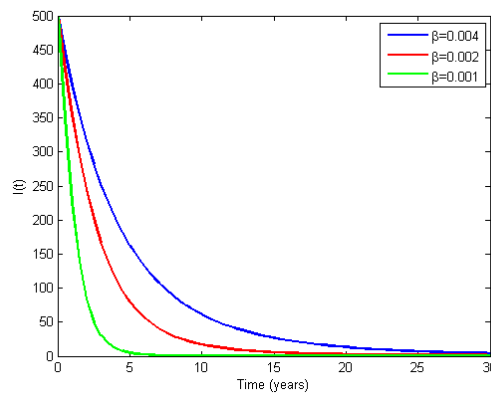


Figure 7. Effect of Contact Rate (β) of the Infected Population $I(t)$

Figure 2 depict the Influence of maternal vaccination φ and treatment rate γ on the basic reproduction. It is observed that increase in both parameters have corresponding

decrease on the basic reproduction number, leading to reduction in the transmission of the disease in the human population.

Figure 3 show the influence of contact rate β and vertical transmission rate θ on the basic reproduction number. It is revealed that increase in both parameters resulted in a matching increase in the basic reproduction number, leading to an increased in the transmission of rubella disease in the human population.

Figure 4 illustrate the impact of first dose of vaccination σ and second dose of vaccination ω on the basic reproduction number. It is observed that increased in both parameters is associated with the reduction in the basic reproduction number. The implication of this is that vaccination will reduce the persistence or prevalence of rubella disease in the human population.

Figure 5 showcase the effect of vertical transmission rate θ and waning out of first vaccination rate ξ on the basic reproduction number. The plot suggested that increased in the values of these parameters leads to increase in the value of the basic reproduction number, resulting to an increase in the spread of rubella disease among the human population.

Figure 6 Confirm that the endemic and disease-free equilibria in infectious human populations are globally asymptotically stable. When the basic reproduction number $R_0 > 1$, the disease will become endemic and persist in the population. This means that regardless of the initial population size, the number of infected individuals will converge to a unique endemic equilibrium point. In other words, the disease will stabilize at a constant level within the population.

Conversely, when the basic reproduction number $R_0 < 1$, the disease will eventually be eradicated from the population. In this scenario, the number of infected individuals will converge to the disease-free equilibrium, regardless of the initial population size. This implies that the number of infected individuals will gradually decline to zero.

Figure 7 shows that as the contact rate β rises, the infected population grows exponentially, demonstrating a direct correlation between the two. This surge in infections can be attributed to the increased interactions among susceptible individuals, creating a higher likelihood of disease transmission. With more frequent contacts, the virus spreads rapidly, contaminating a larger segment of the population. Consequently, the infected class expands, overwhelming healthcare resources. The heightened contact rate fosters an environment conducive to disease propagation, making it challenging to contain outbreaks.

5. CONCLUSION

This study introduces an innovative mathematical framework to investigate rubella transmission dynamics in human populations, incorporating standard incidence rates. Our proposed model undergoes rigorous mathematical analysis, demonstrating epidemiological viability and well-posedness through non-negativity and boundedness of solutions inside a permissible domain Ω .

Our analysis shows that both the disease-free and endemic equilibria are stable. The basic reproduction number R_0 serves as a critical threshold, determining the disease's fate. Specifically:

$R_0 < 1$: Rubella disease is controllable and will be eradicated.

$R_0 > 1$: Rubella persists in the population.

The sensitivity analysis of R_0 reveals the contact rate as the most influential parameter. Strategically administering vaccine does significantly reduce this rate. Additionally, maternal vaccination and recovery rates play crucial roles in mitigating the disease's spread.

Our findings provide valuable insights for policymakers and healthcare professionals, highlighting the importance of vaccination programs targeting high-contact populations, maternal vaccination initiatives, effective recovery and management strategies. By understanding the dynamics of rubella transmission and the impact of key parameters, our research informs evidence-based interventions to control and potentially eliminate this disease.

REFERENCES

- Abdullahi, U., & Sime, S. (2018). The Prevalence of Rubella Virus among Children and Adolescents in Adamawa State, Nigeria. *Journal of Advances in Microbiology*, *11*(3), 1–6.
- Adepoju, O. A., & Ibrahim, H. O. (2024). An optimal control model for monkeypox transmission dynamics with vaccination and immunity loss following recovery. *Healthcare Analytics*, *6*, 100355.
- Adewumi, M. O., Olusanya, R. B., Oladunjoye, B. A., & Adeniji, J. A. (2013). Rubella IgG antibody among Nigerian pregnant women without vaccination history. *African Journal of Clinical and Experimental Microbiology*, *14*(1), 40–44.
- Amelia, D., & Tasman, H. (2021). Mathematics model of measles and rubella with vaccination. *Journal of Physics: Conference Series*, *1725*(1), 12017.
- Bhattacharjee, A., & Jain, K. (2024). Mathematical modelling as a decision making tool to study the COVID-19 pandemic. *AIP Conference Proceedings*, *3139*(1).
- Castillo-Chavez, C., & Song, B. (2004). Dynamical models of tuberculosis and their applications. *Mathematical Biosciences & Engineering*, *1*(2), 361–404.
- Diekmann, O., Heesterbeek, J. A. P., & Metz, J. A. J. (1990). On the definition and the computation of the basic reproduction ratio R_0 in models for infectious diseases in heterogeneous populations. *Journal of Mathematical Biology*, *28*, 365–382.
- Duru, E. C., Anyanwu, M. C., & Nwosu, C. N. (2023). Optimal vaccination and treatment strategies for control of rubella with vertical transmission. *International Journal of Mathematical Analysis and Modelling*, *6*(2).
- Gong, X., Zheng, C., Fang, Q., Xu, W., & Yin, Z. (2024). A case of congenital rubella syndrome and epidemiology of related cases in China, 2014–2023. *Human Vaccines & Immunotherapeutics*, *20*(1), 2334917.
- Oluyo, T. O., & Adeyemi, M. O. (2018). Sensitivity analysis of Zika epidemic model. *Int J Sci Eng Res*, *9*, 587–601.

- Prawoto, B. P., Abadi, A., & Artiono, R. (2020). Dynamic of re-infection Rubella transmission model with vaccination. *AIP Conference Proceedings*, 2264(1).
- Tilahun, G. T., Tolasa, T. M., & Wole, G. A. (2022). Modeling the dynamics of rubella disease with vertical transmission. *Heliyon*, 8(11).
- Van den Driessche, P., & Watmough, J. (2002). Reproduction numbers and sub-threshold endemic equilibria for compartmental models of disease transmission. *Mathematical Biosciences*, 180(1–2), 29–48.
- Vueba, A. N., & do Céu Sousa, M. (2020). Rubella infection: Advances and challenges in the diagnosis and prevention of Congenital Rubella Syndrome. *International Journal of Clinical Virology*, 4(1), 6–13.
- World Health Organization, W. (2011). *Regional office for the Eastern M. Field guidelines for surveillance of measles, rubella and congenital rubella syndrome*. World Health Organization (WHO).
<https://www.who.int/publications/i/item/9789290217428>

Copyrights

Copyright for this article is retained by the author(s), with first publication rights granted to the journal.

This is an open-access article distributed under the terms and conditions of the Creative Commons Attribution license (<http://creativecommons.org/licenses/by/4.0/>).